Brain Mechanisms of Arithmetic: A Crucial Role for Ventral Temporal Cortex

Pedro Pinheiro-Chagas[1,2*], Amy Daitch[2*], Josef Parvizi[2], and Stanislas Dehaene[1,3]

Abstract

■ Elementary arithmetic requires a complex interplay between several brain regions. The classical view, arising from fMRI, is that the intraparietal sulcus (IPS) and the superior parietal lobe (SPL) are the main hubs for arithmetic calculations. However, recent studies using intracranial electroencephalography have discovered a specific site, within the posterior inferior temporal cortex (pITG), that activates during visual perception of numerals, with widespread adjacent responses when numerals are used in calculation. Here, we reexamined the contribution of the IPS, SPL, and pITG to arithmetic by recording intracranial electroencephalography signals while participants solved addition problems. Behavioral results showed a classical problem size effect: RTs increased with the size of the operands. We then examined how high-frequency broadband (HFB) activity is modulated by problem size. As expected from previous fMRI findings, we showed that the total HFB activity in IPS and SPL sites increased with problem size. More surprisingly, pITG sites showed an initial burst of HFB activity that decreased as the operands got larger, yet with a constant integral over the whole trial, thus making these signals invisible to slow fMRI. Although parietal sites appear to have a more sustained function in arithmetic computations, the pITG may have a role of early identification of the problem difficulty, beyond merely digit recognition. Our results ask for a reevaluation of the current models of numerical cognition and reveal that the ventral temporal cortex contains regions specifically engaged in mathematical processing. ■

INTRODUCTION

Elementary arithmetic requires a complex interplay between several brain regions. The classical triple-code model for numerical cognition proposed that the lateral parietal cortex (LPC) hosts the main hubs for numerosity representation and manipulation (Piazza, Pinel, Le Bihan, & Dehaene, 2007; Piazza, Izard, Pinel, Le Bihan, & Dehaene, 2004; Dehaene, Piazza, Pinel, & Cohen, 2003; Pinel, Dehaene, Rivière, & LeBihan, 2001). Indeed, convergent brain imaging, intracranial recording, and stimulation studies have found that the intraparietal sulcus (IPS) is selectively activated (Menon, Rivera, White, Glover, & Reiss, 2000; Stanescu-Cosson et al., 2000) and causally involved in mental arithmetic (Semenza, Salillas, De Pallegrin, & Della Puppa, 2017; Della Puppa et al., 2013). Furthermore, IPS activity has also been shown to increase as problems become harder (Kanjlia, Lane, Feigenson, & Bedny, 2016; De Visscher et al., 2015; De Smedt, Holloway, & Ansari, 2011; Molko et al., 2003; Dehaene, Spelke, Pinel, Stanescu, & Tsivkin, 1999), thus paralleling the classical behavioral problem size effect, which is an increase in calculation time as a function of the magnitude of the operands (Ashcraft, 1992). Moreover,

the superior parietal lobe (SPL) is also activated during calculation (Knops, Thirion, Hubbard, Michel, & Dehaene, 2009), and recent studies have reported that it hosts a topographic map of numerosity (Harvey, Ferri, & Orban, 2017; Harvey, Klein, Petridou, & Dumoulin, 2013).

In addition to the LPC, the triple-code model predicted that the ventral temporal cortex (VTC) would have a key role in number recognition. Indeed, recent studies using intracranial electroencephalography (iEEG) have confirmed the existence of a region in the posterior inferior temporal gyrus (pITG) that selectively activates during visual identification of Arabic numerals (the "number form area" [NFA]), as compared with other similar morphometric symbols, such as letters (Shum et al., 2013). Subsequent iEEG studies have demonstrated that distinct neuronal populations adjacent to the NFA, also within the pITG, respond higher (Hermes et al., 2017) or exclusively (Daitch et al., 2016) to numerals when they are in the context of a calculation and that these pITG sites have high functional connectivity with the IPS (Daitch et al., 2016). These results raised the possibility that pITG might be involved in arithmetic processing beyond visual recognition of mathematical symbols, which is unexpected from previous fMRI and neuropsychological findings, unpredicted by neurocognitive models of arithmetic, and surprising given the traditional view of the VTC as the last stage of the ventral "what"

visual pathway, associated with object categorization (Grill-Spector & Weiner, 2014). However, these prior studies that investigated the role of pITG in arithmetic processing were restricted to either contrasts between numerals and similar morphometric symbols or between calculation and other tasks (e.g., memory/sentence comprehension), thus never testing if, how, and when the activity in pITG is modulated by numerical features of calculations. Consequently, the precise role of pITG in mathematical cognition remains largely elusive.

In this study, we aimed at reevaluating the roles of IPS, SPL, and pITG in mental calculation with an unprecedented level of precision by recording electrophysiological signals directly from the human cortex (iEEG). We asked participants to verify the correctness of visually presented additions, in the form of "13 + 5 = 17," in which we systematically varied the size of the problems (i.e., magnitude of the operands) while preserving the same structure and number of characters, thus separating numerical from low-level visual features of the stimuli.

Based on previous fMRI findings, we predicted that the overall activity in the IPS and SPL would be sustained and increase as a function of problem size. Furthermore, this parametric modulation should be correlated with RT. However, we were less certain about the pITG. If it is only involved in the visual recognition of numerals, we should expect a brief transient burst of activity with no parametric modulation by problem size. But because multidigit calculations might require participants to mentally reevaluate the problem a few times before they reach a final decision, pITG activity may be sustained across the trial and increase as a function of problem size, possibly reflecting the top–down attentional modulation from LPC. Finally, the pITG could be parametrically modulated by problem size, but in a different way and with a different latency as compared with IPS and SPL, thus revealing an unpredicted role in calculation.

METHODS

Participants

We recorded electrocorticography data from 10 patients with epilepsy who were implanted with intracranial electrodes over the VTC and/or LPC as part of their presurgical evaluation at Stanford University Medical Center. Demographic information for each participant is included in Table 2. Each participant was monitored in the hospital for approximately 6–10 days following surgery, during which they participated in our study. Before participating, all participants provided verbal and written consent, which was approved by the Stanford Institutional Review Board. Part of the data of the present cohort was already published elsewhere (Hermes et al., 2017; Daitch et al., 2016; Shum et al., 2013). The inclusion criterion in this study was the completion of at least 80 trials (corresponding to two blocks) of the arithmetic condition to have enough power to investigate parametric modulations within condition (see below).

Behavioral Tasks

Arithmetic and Memory Verification

Participants were asked to verify the correctness of either addition calculations (e.g., "13 + 5 = 17," arithmetic condition) or autobiographical memory statements (e.g., "I ate fruit yesterday," memory condition), visually presented and randomly intermixed within the same block. For the purposes of this study, the "memory condition" served as a sentence/language comprehension control condition for arithmetic. Additions were always composed of a two-digit operand (ranging from 10 to 87), a one-digit operand (ranging from 1 to 9, excluding 3) in either order, and a two-digit proposed result (Table 1). In half of the trials, the proposed result was correct. The absolute deviant for the incorrect proposed results ranged from 1 to 16. Participants responded in the self-paced manner by pressing one of two keypad buttons. The trials were

Table 1. Stimuli List for the Arithmetic Task

10 + 1 = 11	78 + 2 = 80	4 + 25 = 29	5 + 87 = 92	56 + 6 = 62	24 + 7 = 31	16 + 8 = 24	45 + 9 = 54
1 + 18 = 19	78 + 2 = 65	4 + 25 = 32	5 + 87 = 93	56 + 6 = 64	26 + 7 = 33	16 + 8 = 22	45 + 9 = 55
1 + 18 = 25	2 + 52 = 54	24 + 5 = 29	28 + 6 = 34	67 + 6 = 73	26 + 7 = 34	47 + 8 = 55	47 + 9 = 56
1 + 41 = 42	2 + 52 = 56	24 + 5 = 39	28 + 6 = 36	6 + 22 = 28	59 + 7 = 66	47 + 8 = 54	47 + 9 = 56
1 + 41 = 50	2 + 60 = 62	33 + 5 = 38	38 + 6 = 44	6 + 22 = 33	59 + 7 = 65	8 + 30 = 38	53 + 9 = 62
11 + 2 = 16	2 + 60 = 72	33 + 5 = 32	38 + 6 = 42	6 + 36 = 42	7 + 34 = 41	8 + 30 = 45	53 + 9 = 63
24 + 2 = 26	20 + 4 = 24	81 + 5 = 86	42 + 6 = 48	6 + 36 = 43	7 + 34 = 42	8 + 65 = 73	9 + 23 = 32
24 + 2 = 19	20 + 4 = 17	81 + 5 = 92	42 + 6 = 59	6 + 39 = 45	7 + 43 = 50	8 + 65 = 74	9 + 23 = 34
61 + 2 = 63	54 + 4 = 58	5 + 63 = 68	51 + 6 = 57	6 + 39 = 47	7 + 43 = 63	44 + 9 = 53	9 + 86 = 95
61 + 2 = 75	54 + 4 = 65	5 + 63 = 56	51 + 6 = 71	24 + 7 = 31	7 + 67 = 73	44 + 9 = 51	9 + 86 = 96

interspersed with fixation periods (5 or 10 sec), during which participants were simply asked to fixate at a crosshair in the center of the screen. A 200-msec intertrial interval (ITI) separated trials. All participants but one verified 80 additions and 50 memory statements (Participant S1 evaluated 120 additions and 100 memory statements), divided in two blocks of 40 additions and 25 memory statements each.

Symbol Identification

Participants were visually presented with a series of symbols falling under one of three categories: (1) Arabic numerals (ranging from 1 to 9), (2) letters in the Latin alphabet (A, C, D, E, H, N, R, S, or T), or (3) letters in foreign alphabets. Each category had 72 trials randomly shuffled and divided in two blocks. For each symbol, participants had to press a given button if they could read the symbol (i.e., numbers or letters in the Latin alphabet) and another button if they could not read it (i.e., symbols in foreign alphabets). Participants had up to 15 sec to respond to each stimulus, and trials were separated by a 500-msec ITI. The tasks were presented on a laptop computer (Apple MacBook or MacBook Pro), using MATLAB's Psychtoolbox (Brainard, 1997).

Electrodes

Each participant was implanted with grids and/or strips of subdural platinum electrodes (AdTech Medical Instruments Corporation), whose locations were determined purely for clinical reasons. Each electrode had an exposed diameter of 2.3 mm, with interelectrode spacing of 10, 7, or 5 mm for higher density arrays.

Electrode Localization

Electrode locations were mapped on each participant's own cortical surface with the following steps: (1) A postsurgical CT (with electrodes) was aligned to a presurgical T1-weighted MRI using SPM8 (www.fil.ion.ucl.ac.uk/spm/). (2) Electrode coordinates were manually localized within the aligned CT as the center of high image intensity spheres. (3) The identified electrode coordinates were adjusted for minor cortical shifts following surgery, with a local projection defined separately for each grid or strip (Hermes, Miller, Noordmans, Vansteensel, & Ramsey, 2010). (4) Cortical surface reconstructions of each participant's brain were obtained by manually segmenting the white matter from the participant's T1-weighted MRI using ITKGray (vistalab.stanford.edu/newlm/index.php/ItkGray) and growing out two layers of gray matter from the white matter surface. Finally, electrodes were labeled by an expedient neuroanatomist based on the subdivision of LPC and VTC shown in Figure 1. For group plots, each participant's electrode coordinates, defined in native brain space, were realigned to a normalized brain (MNI Colin 27, www.bic.mni.mcgill.ca/ServicesAtlases/Colin27), and coordinates across participants were plotted in this common space. Note that the location of each electrode site projected in MNI space may look slightly different (relative to gyral landmarks, etc.) than in native space and was done purely for visualization purposes. Anatomical parcellations within the VTC and LPC were determined based on each participant's own gyral landmarks in native brain space.

Data Acquisition and Analysis

iEEG data were recorded from subdural electrodes via a multichannel recording system (Tucker David Technologies). Data were acquired with a band pass filter of 0.5–300 Hz and sampling rate of 1525.88 Hz. An electrode outside the seizure zone with the most silent electrocorticographic activity was selected as an online reference during acquisition.

Preprocessing

First, electrodes with epileptiform activity or those corrupted by electrical noise were eliminated from subsequent analyses. Electrodes were also excluded—those whose overall power was 5 or more standard deviations above or below the mean power across channels and those whose power spectrum strayed from the normal $1/f$ power spectrum based on visual inspection. All nonexcluded channels were then notch-filtered at 60 Hz and harmonics to remove electric interference, then rereferenced to the mean of the filtered signals of the nonexcluded channels. The rereferenced signal at each electrode was then band-pass filtered between 70 and 180 Hz (high-frequency broadband [HFB]) using sequential 10-Hz width band-pass windows (70–80 Hz, 80–90 Hz, etc.), using two-way, zero-lag, finite impulse response filters. The instantaneous amplitude of each band-limited signal was computed by taking the modulus of the Hilbert transform signal. The amplitude of each 10-Hz band signal was normalized by its own mean; then these normalized amplitude time series were averaged together, yielding a single amplitude time course for the HFB band.

Task-related HFB Changes

Our analyses were focused on task-induced changes in HFB activity (70–180 Hz) because of its high correlation with local spiking activity and the fMRI BOLD signal (Foster, Rangarajan, Shirer, & Parvizi, 2015; Parvizi et al., 2012; Ray & Maunsell, 2011; Manning, Jacobs, Fried, & Kahana, 2009; Logothetis, Pauls, Augath, Trinath, & Oeltermann, 2001). For the arithmetic and memory verification task, we first identified electrodes within the VTC and LPC that responded selectively during arithmetic calculations relative to reading sentences comprehension/memory retrieval. We classified all sites
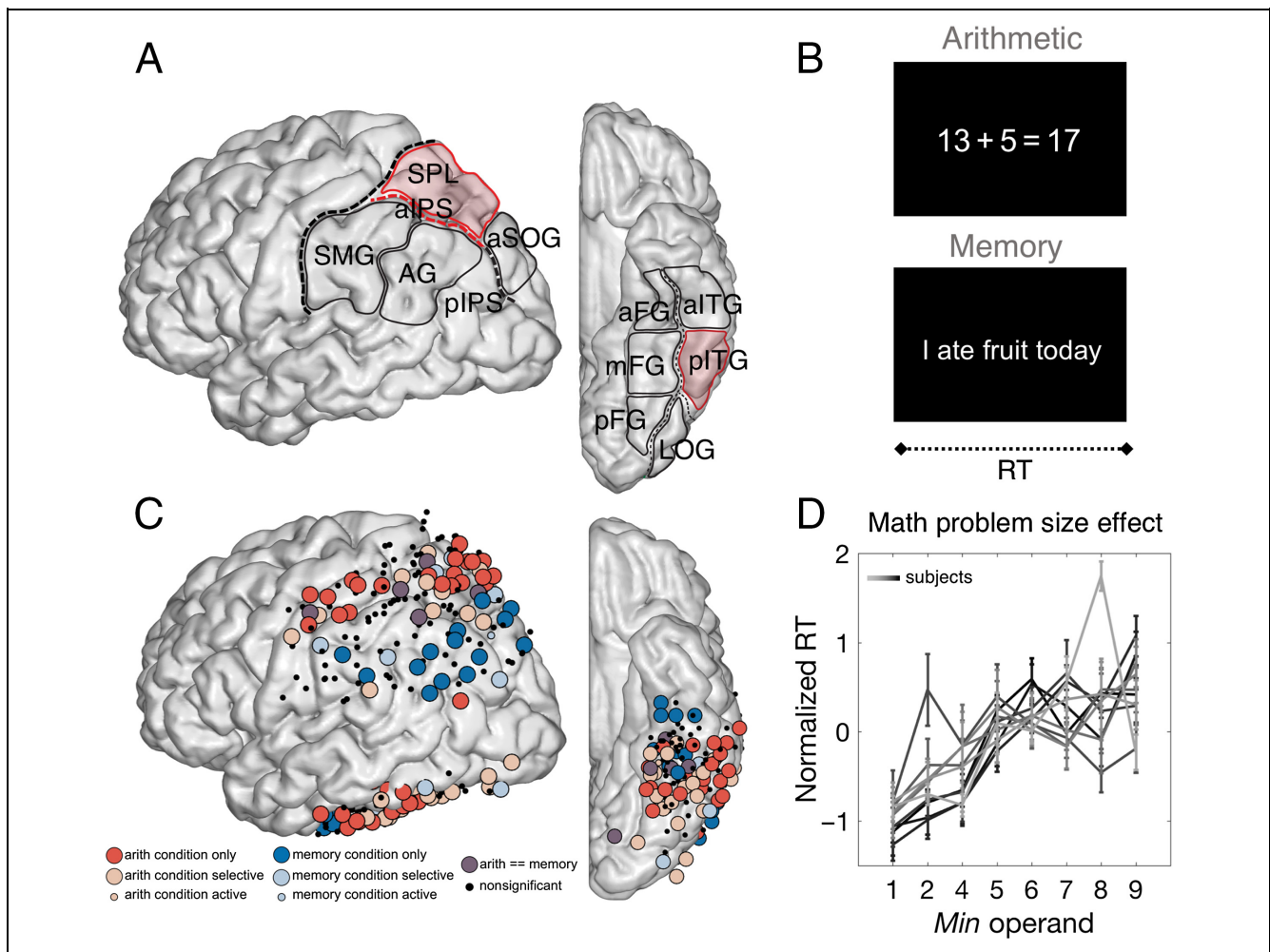
Figure 1. Anatomical subdivisions, task, recording sites, and behavioral problem size effect. (A) The anatomical subdivisions within the LPC and VTC considered in this study, as seen in the left hemisphere from a slightly posterior viewpoint. LPC: AG, angular gyrus; aSOG, anterior superior occipital gyrus; pIPS posterior IPS; SMG, supramarginal gyrus. VTC: aFG, anterior fusiform gyrus; aITG, anterior inferior temporal gyrus; pFG, posterior fusiform gyrus; mFG, mid fusiform gyrus. Arithmetic ROIs marked in red. (B) Exemplar stimuli of the memory and arithmetic verification task. In each trial, participants were asked to verify the correctness of visually presented additions or memory statements by pressing one of two buttons. (C) LPC and VTC sites from all 10 participants are projected onto a single left hemisphere using the MNI space (see Electrode Localization in the Methods), with the color of each site indicating its selectivity for arithmetic versus memory. Bright blue and bright red mark the most selective sites, passing three criteria for significance (e.g., arithmetic > baseline, arithmetic > memory, and memory indistinguishable from baseline). Faded red and blue indicate the selective sites that met only the first two criteria. Small faded red and blue indicate sites that met only the first criteria. Sites colored in purple were activated similarly during the two conditions, and sites marked by small black dots were not significantly active during either condition. Significance was defined as $p < .05$, FDR-corrected within participant. (D) Behavioral problem size effect (*min* operand) in each participant (different shades of gray): average RT plotted as a function of *min* operand (normalized within each participant by subtracting the mean and dividing by the standard deviation).

into six groups based on their relative responses during arithmetic versus memory trials. (1) "Arithmetic active" channels were defined as those with significantly greater HFB activity during arithmetic trials (0–1000 msec following stimulus onset) than during baseline (200 msec ITI). (2) "Arithmetic-selective" channels satisfied 1 and also exhibited significantly greater HFB activity during arithmetic than memory trials (0–1000 msec following stimulus onset for each condition). (3) "Arithmetic-only" channels satisfied 1 and 2 and additionally exhibited no significant increase in activity during memory trials (0–1000 msec following stimulus onset). (4–6) "Memory-active," "memory-selective," and "memory-only" channels were classified

using equivalent criteria as 1–3, but comparing activity during memory trials to that during baseline or arithmetic trials. For the symbol identification task, a similar procedure was used to determine channel selectivity, but using a time window of 0–400 msec after stimuli onset and a baseline of −200 msec before stimuli onset. Channels were classified as (1) "numeral active" if they showed significantly greater HFB activity during numerals identification as compared with baseline and (2) "numeral selective" if they satisfied 1 and also exhibited significantly greater HFB activity during numerals identification as compared with Latin and foreign letters. Unpaired permutation tests were run to test for differences in HFB power

between different task conditions, whereas paired permutation tests were run to test for a difference in HFB power between a task condition and baseline. All p values in all analyses were false discovery rate (FDR)-corrected by the total number of VTC and LPC channels within each participant.

RESULTS
Behavior Results

Accuracy for the arithmetic condition was high (80% or higher) in 9 of 10 participants (Table 2). To model RTs in each participant, we calculated stepwise regression models with the smaller operand (*min*), the larger operand (*max*), the sum, and the absolute deviant as predictors. Results revealed that the *min* operand was a significant and the best predictor of RT in 9 of 10 participants (βs > 0.32, p < .003), whereas the sum and the absolute deviant were significant predictors only in two participants (βs > 0.28, p < .01). The *max* operand was not a significant predictor of RT in any model (Table 3).

These behavioral results corroborate previous findings using a variety of paradigms, such as verification (Groen & Parkman, 1972), production (Uittenhove, Thevenot, & Barrouillet, 2016; Barrouillet & Thevenot, 2013), and number-to-position (Pinheiro-Chagas, Dotan, Piazza, & Dehaene, 2017) in which the *min* operand was also found to be the best predictor of RT (Pinheiro-Chagas et al., 2017; Uittenhove et al., 2016; Barrouillet & Thevenot, 2013; Groen & Parkman, 1972), thus providing convergent evidence that the *min* operand is a robust and reproducible index of problem size/difficulty.

Selectivity for Arithmetic in pITG, anterior IPS, and SPL Sites

Next, we investigated the arithmetic versus memory selectivity in several recording sites across all participants. We found that our arithmetic ROIs—pITG, anterior IPS (aIPS), and SPL—were highly selective to arithmetic processing, as previously reported (Hermes et al., 2017; Daitch et al., 2016) and in line with a recent fMRI study that used an analogous task (Amalric & Dehaene, 2016). Forty percent of sites within the pITG (11/28), 21% of sites around the aIPS (7/33), and 25% of sites within the SPL (13/53) responded exclusively during the arithmetic condition (Figure 1C). Moreover, most of the arithmetic-selective sites in these regions exhibited sustained activity during the computation. In sharp contrast, the memory condition produced activity in the language network including LPC regions such as the angular gyrus and STS (Pallier, Devauchelle, & Dehaene, 2011) and in more medial portions of the inferior temporal cortex, close to the visual word form area (Hannagan, Amedi, Cohen, Dehaene-Lambertz, & Dehaene, 2015). Nonselective sites showed either transient activity following stimulus onset in both conditions, likely involved in the visual processing of the stimulus, or later activity just before participants' motor response, probably engaged in motor planning.

Parametric Modulation of HFB Power by *Min* Operand in pITG, aIPS, and SPL

Given the behavioral evidence that the *min* operand was the best index of problem size/difficulty, we next investigated if, how, and when the *min* operand modulated the

Table 2. Participant Demographics and Behavioral Performance

Participant	Sex	Age	IQ	Handedness	Hemi	Behavior Performance		
						Arith Acc (%)	Avg Arith RT (sec)	Avg Memory RT (sec)
S1	M	41	129	R	R	96	3.18	2.15
S2	F	36	N/A	R	L	95	3.69	2.1
S3	F	22	N/A	R	L	89	5.78	3.12
S4	M	46	N/A	A	R	93	5.24	3.38
S5	F	31	71	R	L	63	3.61	3.11
S6	M	29	77	R	L	88	2.85	3.13
S7	M	47	74	L	L	96	3.3	3.23
S8	M	67	N/A	R	R	94	2.02	2.84
S9	F	65	113	R	R	80	3.28	2.35

This table shows the sex, age at time of surgery, IQ (N/A indicates that the IQ test was not performed before surgery), handedness (R = right-handed; L = left-handed; A = ambidextrous), and Hemi (hemisphere of coverage) of all individuals participating in study. It also shows the accuracy and average RT for each condition (arithmetic and memory). Arith ACC = arithmetic accuracy; Avg Arith RT = averaged arithmetic reaction time; Avg Memory RT = averaged memory reaction time.

Table 3. Arithmetic Problem Size Effect by Participant

Participant	Min Operand				Max Operand				Sum				Absolute Deviant			
	β	In	t	p	β	In	t	p	β	In	t	p	β	In	t	p
S1	0.45	✓	5.55	1.7E−07	0.08	–	0.99	.32	−0.02	–	−0.29	.78	0.08	–	0.99	.32
S2	0.58	✓	6.30	1.6E−08	0.08	–	0.82	.41	0.05	–	0.52	.60	0.08	–	0.82	.41
S3	0.71	✓	8.76	3.5E−13	0.13	–	1.68	.10	0.03	–	0.34	.74	0.14	–	1.68	.10
S4	0.40	✓	4.11	1.0E−04	0.00	–	0.00	1.00	0.16	–	1.61	.11	0.31	✓	3.15	2.4E−03
S5	0.05	–	0.41	0.68	−0.01	–	−0.07	.94	0.29	✓	2.63	1.0E−02	0.00	–	−0.02	.98
S6	0.32	✓	3.01	3.5E−03	0.07	–	0.69	.49	0.02	–	0.16	.87	0.08	–	0.69	.49
S7	0.47	✓	4.43	3.1E−05	0.12	–	1.16	.25	0.15	–	1.36	.18	0.12	–	1.16	.25
S8	0.37	✓	3.58	6.1E−04	0.00	–	0.00	1.00	0.31	✓	3.05	3.2E−03	0.29	✓	2.92	4.7E−03
S9	0.44	✓	4.01	1.4E−04	−0.10	–	−0.96	.34	0.04	–	0.31	.88	−0.01	–	−0.96	.34
S10	0.53	✓	5.38	8.1E−07	0.00	–	0.00	1.00	−0.15	–	−1.44	.15	0.15	–	1.67	.09

This table shows the statistics of the stepwise regression analysis, which included the RT as the dependent variable and the *min* operand, *max* operand, sum, and absolute deviant as predictors. "In" indicates if the predictor was included (✓, $p < .05$) or not (–) in the final model.

activity in our arithmetic ROIs. To do so, we performed linear regression analysis on the HFB activity at each recording site on two time windows: initial activity (averaged power over 0–1,000 msec following stimulus onset, where greater activity was observed) and total activity (the integral—area under the curve—from stimulus onset to participant's RT).

As expected from previous fMRI findings, the total activity increased as a function of *min* operand in several aIPS (5/12 sites, 42% in 3/7 participants with aIPS coverage) and SPL (7/17 sites, 41% in 3/7 participants with SPL coverage) sites ($p < .05$, FDR-corrected; Table 4; Figures 2A, 3, and 5A). Importantly, no site in pITG showed this effect.

Table 4. Number of Electrodes Showing Arithmetic Selectivity and Modulation by the *Min* Operand, by Participant/Anatomical Region

Participant	Hemi	pITG						aIPS						aSPL					
		TOT	AA	AS	AO	DecIN	IncTO	TOT	AA	AS	AO	DecIN	IncTO	TOT	AA	AS	AO	DecIN	IncTO
S1	R	5	3	3	3	3,3,3	–,–,–	6	2	2	2	–,–,–	–,–,–	8	3	2	1	–,–,–	–,–,–
S2	L	2	2	2	–	1,1,–	–,–,–	4	2	2	–	1,1,–	2,2,–	8	6	5	3	1,1,1	4,4,2
S3	L	–	–	–	–	–,–,–	–,–,–	3	2	1	–	–,–,–	2,1,–	7	2	2	1	–,–,–	2,2,1
S4	R	–	–	–	–	–,–,–	–,–,–	4	2	2	2	–,–,–	1,1,1	7	1	1	1	–,–,–	1,1,1
S5	L	3	2	2	1	2,2,1	–,–,–	–	–	–	–	–,–,–	–,–,–	5	2	2	2	1,1,1	–,–,–
S6	L	5	4	2	1	1,1,1	–,–,–	5	3	3	2	1,1,1	–,–,–	12	5	5	5	–,–,–	–,–,–
S7	L	4	1	1	1	–,–,–	–,–,–	4	–	–	–	–,–,–	–,–,–	5	–	–	–	–,–,–	–,–,–
S8	R	6	5	5	3	2,2,2	–,–,–	–	–	–	–	–,–,–	–,–,–	–	–	–	–	–,–,–	–,–,–
S9	R	3	2	2	2	1,1,1	–,–,–	4	2	1	–	–,–,–	–,–,–	1	–	–	–	–,–,–	–,–,–
S10	L	–	–	–	–	–,–,–	–,–,–	3	1	1	1	–,–,–	–,–,–	–	–	–	–	–,–,–	–,–,–
Total		28	19	17	11	10,10,8	–,–,–	33	14	12	7	2,2,1	5,4,1	53	19	17	13	2,2,2	7,7,4

The numbers separated by commas correspond to AA, AS, AO, respectively. Electrodes included are statistically significant at $p < .05$, FDR-corrected within participants. Hemi = hemisphere; TOT = total number of electrodes; AA = arithmetic condition active (relative to baseline); AS = arithmetic condition selective (relative to baseline and memory); AO = arithmetic condition only (arithmetic-selective and memory not active relative to baseline); DecIN = decreased initial activity as a function of *min* operand; IncTO = increased total activity as a function of *min* operand.
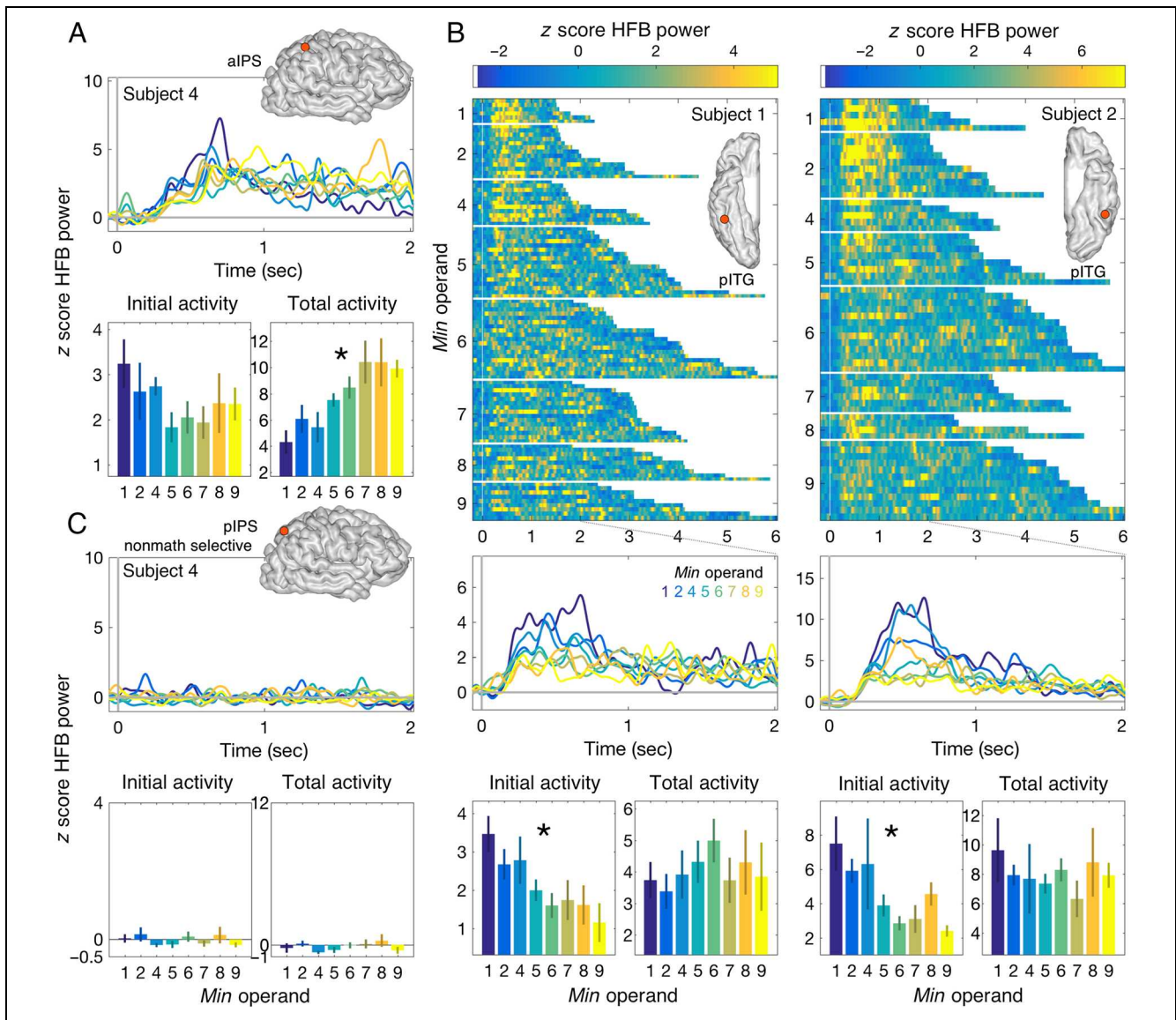
Figure 2. Example sites whose activity is modulated by the *min* operand. (A) Exemplar arithmetic-selective channel in the aIPS showing increased HFB total activity as a function of *min* operand. The time course shows the activity averaged across trials with a given *min* operand (zoomed in the first 2 sec of the trial). Bar plots show average initial activity (within the first second of a trial) and average total activity (integrated over the whole trial) as a function of *min* operand. (B) Two exemplar channels showing decreased HFB initial activity in the pITG as a function of *min* operand (both arithmetic-selective, one in each hemisphere in two different participants). The first plot in each column shows the time course of activity for each trial, sorted by *min* operand and then by RT. (C) Exemplar channel of a nonarithmetic-selective channel in the posterior IPS of the same participant as in B, showing no HFB modulation by *min* operand. An asterisk indicates that a regression analysis found a significant effect of *min* operand on either initial or total HFB activity ($p < .05$, FDR-corrected).

Surprisingly, however, we found that the initial activity significantly decreased as a function of *min* operand ($p < .05$, FDR-corrected) in several arithmetic-selective pITG sites (10/17, 59% in 6/7 participants with pITG coverage) and in one anterior ITG site, just adjacent to the pITG (Table 4). Examples of activation profiles at the single trial level are shown in Figure 2B (see also Figures 4 and 5A). This proportion increased when considering only the arithmetic-selective channels that did not show any significant response during the memory condition (arithmetic-only channels: 8/11, 72%).

The same effect was also observed in a small proportion of the arithmetic-selective channels in the aIPS and SPL (aIPS: 2/12, 17% in 2/7 participants with aIPS coverage; SPL: 2/17 sites, 12% in 2/7 participants with SPL coverage). But as can be seen in Figure 5A, the pattern of modulation by problem size/difficulty is overall highly dissociable between and arithmetic-selective ITG in aIPS/SPL sites. Indeed, the effect of *min* operand in the initial activity was much higher (negative sign) for the ITG sites that showed a significant decrease in the initial activity as compared with the aIPS/SPL sites that showed a significant
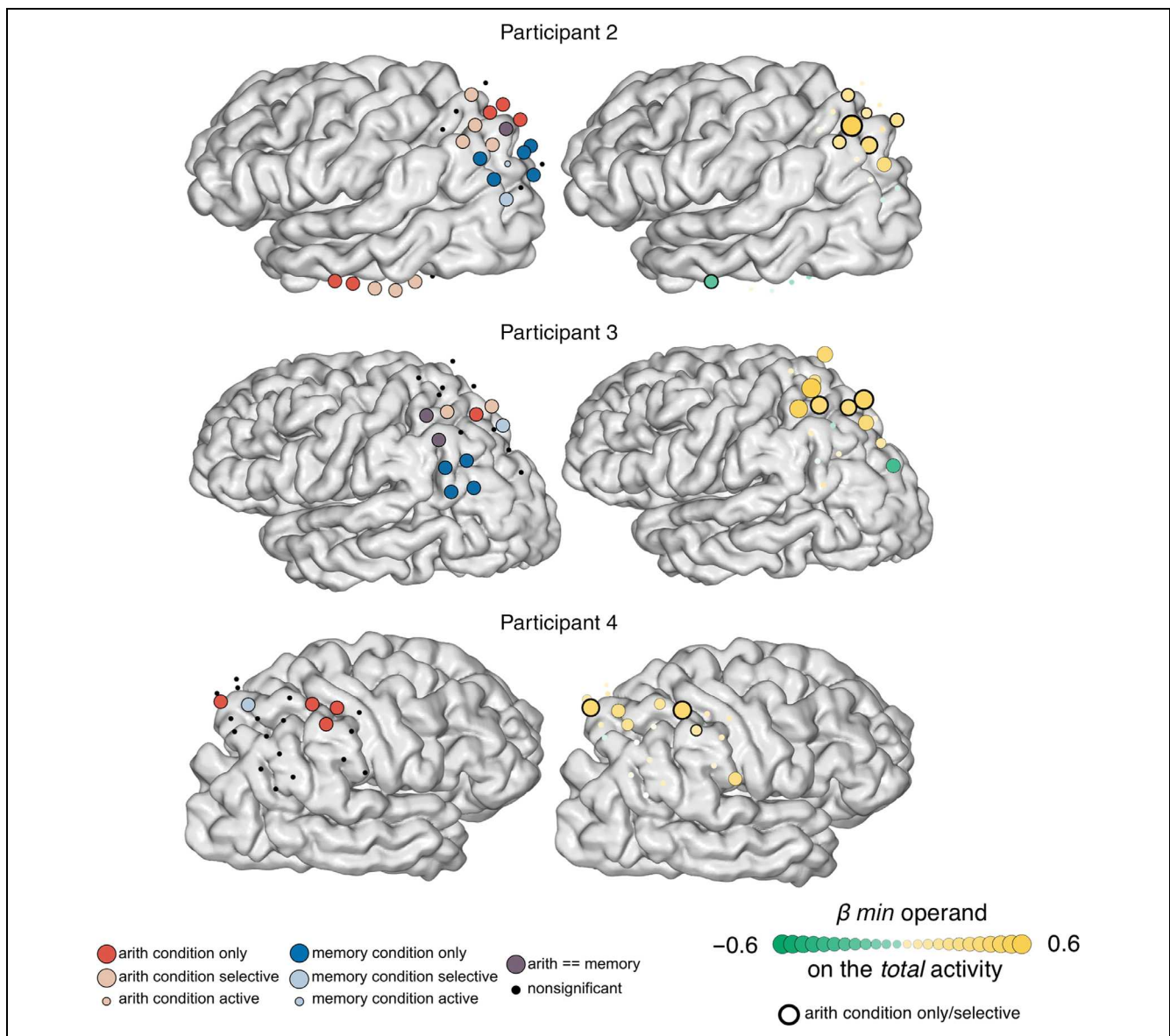
Figure 3. Anatomical and functional specificity of the HFB activity modulation in the LPC. The figure illustrates the relationship, in LPC, between (1) selectivity for arithmetic versus memory (left brain, same color code as Figure 1B) and (2) the effect of the *min* operand on total activity (right brain). The figure shows all three (out of seven) participants with LPC coverage who showed the effect. Most channels whose total activity increased with problem size were located within the aIPS and SPL and were arithmetic-selective, but some channels that showed this effect felt outside aIPS and SPL and/or were not arithmetic-selective. For the *min* effect, dot color indicates the size and sign of the regression coefficient, and dot size indicates the size of the regression coefficient. A thick black ring indicate that the channel is also arithmetic-selective. Small dots indicate nonsignificant channels. *p* Values were FDR-corrected within participant.

increase in total activity (mean β in ITG = −0.3828, *SD* = 0.0619; mean β aIPS/SPL = −0.104, *SD* = 0.143; *t*(21) = −5.932, *p* < .001). Conversely, the effect of *min* operand in the total activity was much higher for the aIPS/SPL sites that showed a significant increase in the total activity as compared with the ITG sites that showed a significant decrease in the initial activity (mean β in aIPS/SPL = 0.422, *SD* = 0.077; mean β aIPS/SPL = −0.056, *SD* = 0.1538; *t*(21) = 9.562, *p* < .001).

To evaluate the specificity of these results, we next analyzed functional control sites, where activity was memory-selective or equally responsive to arithmetic and memory

(Table 5), as well as anatomical control sites (arithmetic-selective channels that were outside our arithmetic ROIs; Table 6). None of the memory-selective channels nor channels that equally responded to arithmetic and memory across any brain region showed a significant decrease in the initial HFB activity as a function of *min* operand. Very few nonarithmetic-selective channels in the ROIs showed an increase of total HFB activity as a function of *min* operand.

Likewise, very few arithmetic-selective channels located outside the ROIs showed either a decrease in the initial HFB activity or an increase in the total HFB activity as a function of *min* operand.

In summary, parametric modulations were almost entirely dissociated into two categories, found in both left and right hemispheres (Figure 5): (1) decreases in initial activity with increasing *min* operand, showing a high specificity to arithmetic-selective sites mostly in pITG, and (2) increases in total activity with increasing *min* operand in aIPS and SPL arithmetic-selective sites.

Specificity of the pITG Modulation to Calculation

Was the pITG modulation due to calculation itself? An alternative possibility is that this is a visual recognition effect. The smaller a numeral is, the higher is its frequency in spoken and written language (Dehaene & Mehler, 1992). Thus, visual frequency (greater activation to frequent digits) rather than calculation difficulty could drive the pITG effect. However, this would predict that the effect should be found whenever participants process digits, even in the absence of any calculation.

To test whether the modulation observed in the pITG by the magnitude of the *min* operand was present in any context or exclusively during arithmetic calculations, we analyzed the data of the symbol identification task. First, we investigated the selectivity to symbols in the ITG sites that showed decreased activity as a function of *min* operand. We found that 7 of 11 sites were active, but not selective to Arabic numerals, that is, they equally responded to Latin and foreign letters (Table 7). And the remaining four sites were not even active for any symbol. Only one site showed selectivity for numerals, thus qualifying for belonging to the NFA (Shum et al., 2013). Those findings
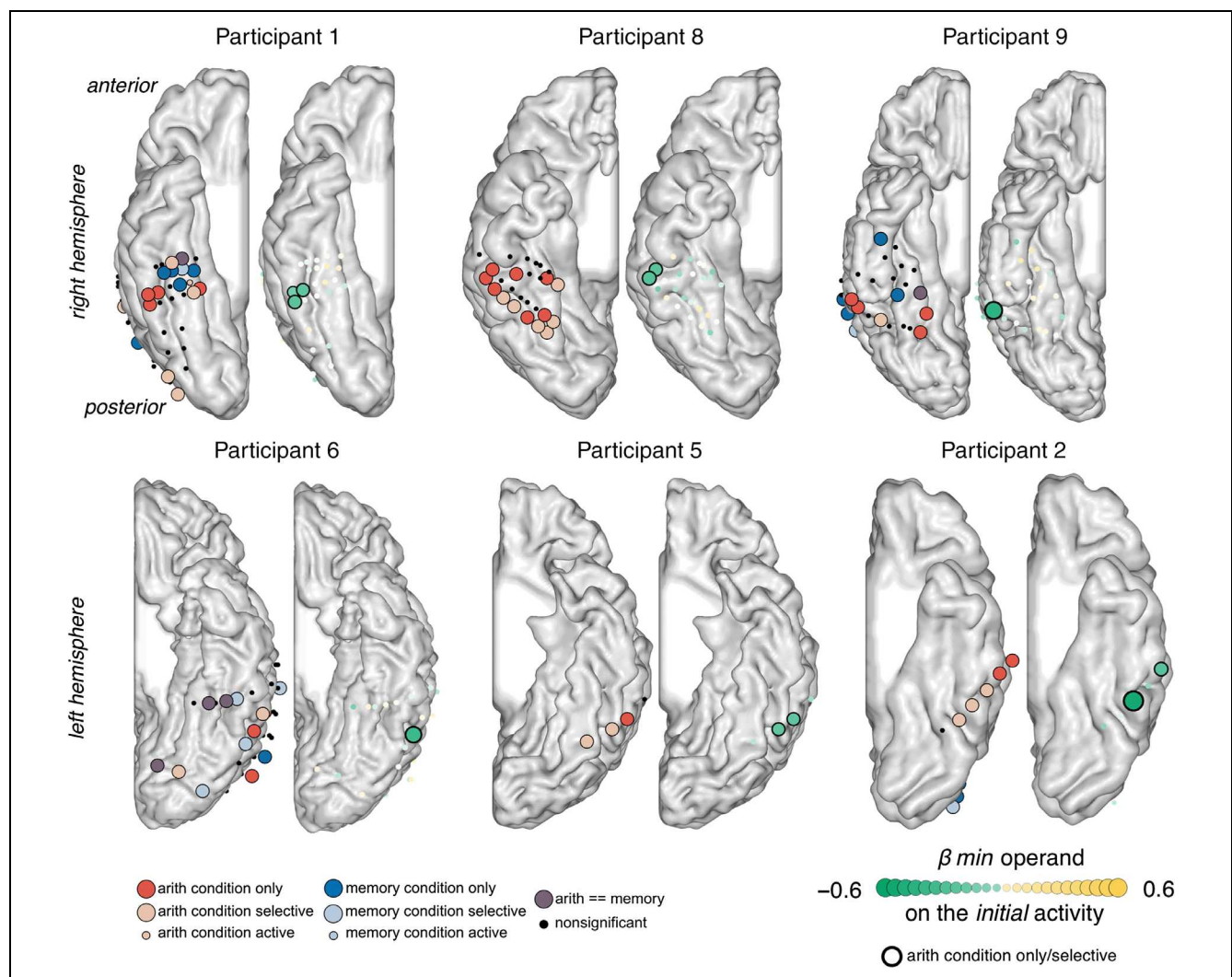

Figure 4. Anatomical and functional specificity of the HFB activity modulation in the VTC. The figure illustrates the relationship, in VTC, between (1) selectivity for arithmetic versus memory (left brain, same color code as Figure 1B) and (2) the effect of the *min* operand on initial activity (right brain). The figure shows all six (out of seven) participants with pITG coverage who showed the effect. All channels whose initial activity decreased with problem size were located within the pITG (except for the most anterior channel of Participant 2—anterior ITG—and were arithmetic-selective (thick black ring). For the *min* effect, dot color indicates the size and sign of the regression coefficient, and dot size indicates the size of the regression coefficient (standardized; $p < .05$, FDR-corrected). Small dots indicate nonsignificant channels.
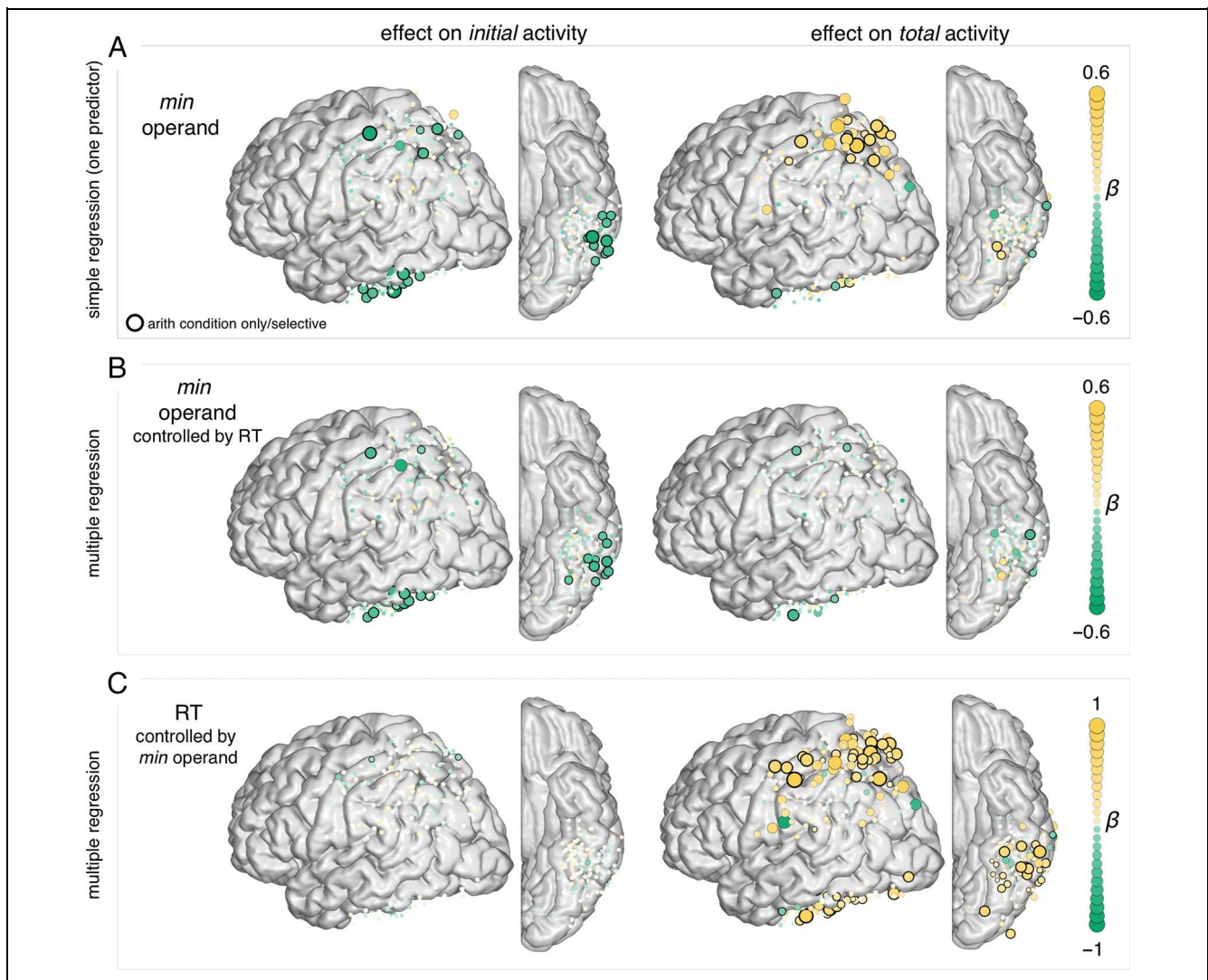
Figure 5. Modulation by *min* operand and RT in the LPC and VTC. Regression analysis, where activity is modeled as a function of *min* operand in the initial activity (within the first second of a trial, left column) and total activity (integrated over the whole trial, right column). (A) The effect of the *min* operand in a simple regression (one predictor). (B) The effect of the *min* operand in a multiple regression that included both the *min* operand and the RT as predictors. (C) The effect of the RT in a multiple regression that included both the *min* operand and the RT as predictors. For all plots, dot color indicates the size and sign of the regression coefficient, and dot size indicates the size of the regression coefficient significant (standardized). A thick black ring indicate that the channel is also arithmetic-selective. Small dots indicate nonsignificant channels. Significance: $p < .05$, FDR-corrected.

fit with recent evidence that the NFA occupies a small ventral occipitotemporal site and that many more lateral sites respond to calculation itself rather than mere digit recognition (Grotheer, Jeska, & Grill-Spector, 2018; Daitch et al., 2016).

Next, we performed a linear regression analysis on the averaged HFB power during symbol identification, between 0 and 500 msec, the window where the highest activity was observed, with the Arabic numerals (ranging from 1 to 9) as predictors. None of the 11 sites showed a significant positive or negative effect of number magnitude ($p > .1$, FDR-corrected for only the 11 channels, to be more liberal). Therefore, the engagement and selectivity to mathematical objects/processing in the ITG was much more selective during calculation as compared with digit

recognition and, crucially, the parametric modulation by number magnitude (*min* operand) was exclusively present during calculation.

Other Potential Confounds

The list of arithmetic problems used in our study were not constructed with the problem size effect in mind, and the *min* variable may therefore be confounded with other variables. In particular, we thank one of the anonymous reviewers for spotting that "number of unique digits" had a small positive correlation with *min* operand ($\rho = 0.23$, $p = .041$; e.g., $10 + 1 = 11$ has two unique digits, whereas $47 + 9 = 56$ has five). If the ITG sites were purely engaged in digit recognition, their activity

Table 5. Number of Electrodes Showing Memory Selectivity and Modulation by the *Min* Operand, by Participant/Anatomical Region

		pITG						aIPS						SPL					
Participant	Hemi	TOT	MA	MS	MO	DecIN	IncTO	TOT	MA	MS	MO	DecIN	IncTO	TOT	MA	MS	MO	DecIN	IncTO
S1	R	5	–	–	–	–,-,-	–,-,-	6	–	–	–	–,-,-	–,-,-	8	3	1	–	–,-,-	–,-,-
S2	L	2	2	–	–	1,-,-	–,-,-	4	3	1	1	1,-,-	2,-,-	8	3	–	–	–,-,-	2,-,-
S3	L	–	–	–	–	–,-,-	–,-,-	3	1	–	–	–,-,-	1,-,-	7	1	–	–	–,-,-	1,-,-
S4	R	–	–	–	–	–,-,-	–,-,-	4	–	–	–	–,-,-	–,-,-	7	1	1	–	–,-,-	1,1,-
S5	L	3	1	–	–	1,-,-	–,-,-	–	–	–	–	–,-,-	–,-,-	5	–	–	–	–,-,-	–,-,-
S6	L	5	2	2	–	–,-,-	–,-,-	5	–	–	–	–,-,-	–,-,-	12	–	–	–	–,-,-	–,-,-
S7	L	4	–	–	–	–,-,-	–,-,-	4	–	–	–	–,-,-	–,-,-	5	–	–	–	–,-,-	–,-,-
S8	R	6	2	–	–	–,-,-	–,-,-	–	–	–	–	–,-,-	–,-,-	–	–	–	–	–,-,-	–,-,-
S9	R	3	–	–	–	–,-,-	–,-,-	4	1	–	–	–,-,-	–,-,-	1	–	–	–	–,-,-	–,-,-
S10	L	–	–	–	–	–,-,-	–,-,-	3	–	–	–	–,-,-	–,-,-	–	–	–	–	–,-,-	–,-,-
Total		28	7	2	–	2,-,-	–,-,-	33	5	1	1	1,-,-	3,-,-	53	8	2	–	–,-,-	4,1,-

The numbers separated by commas correspond to MA, MS, MO, respectively. Electrodes included are statistically significant at $p < .05$, FDR-corrected within participants. Hemi = hemisphere; TOT = total number of electrodes; MA = memory condition active (relative to baseline); MS = memory condition selective (relative to baseline and arithmetic); MO = memory condition only (memory selective and arithmetic not active relative to baseline); DecIN = decreased initial activity as a function of *min* operand; IncTO = increased total activity as a function of *min* operand.

could be lower for trials with fewer distinct digits, thus potentially explaining the *min* effect. To evaluate this possibility, we used a multiple regression approach. First, we excluded trials with only two unique digits because they were only present in problems with *min* operand = 1. This already reduced the correlation between NUD and *min* operand to $\rho = 0.20$, $p = .08$. Next, we ran a multiple regression model with *min*

Table 6. Number of Electrodes Showing Modulation by the *Min* Operand by Participant in Other Anatomical Regions

		Other Anatomical Regions (outside pITG, aIPS, and SPL)										
Participant	Hemi	TOT	AA	AS	AO	DecIN	IncTO	MA	MS	MO	DecIN	IncTO
S1	R	45	10	7	2	1,1,1	–,-,-	10	7	6	–,-,-	–,-,-
S2	L	12	3	3	2	1,1,1	–,-,-	7	5	4	–,-,-	1,-,-
S3	L	9	1	–	–	–,-,-	–,-,-	6	5	4	–,-,-	–,-,-
S4	R	11	1	1	1	–,-,-	1,1,1	–	–	–	–,-,-	–,-,-
S5	L	1	1	1	–	–,-,-	–,-,-	1	–	–	–,-,-	–,-,-
S6	L	26	8	3	1	–,-,-	–,-,-	7	3	1	–,-,-	–,-,-
S7	L	9	2	2	1	–,-,-	–,-,-	–	–	–	–,-,-	–,-,-
S8	R	20	8	8	4	–,-,-	2,2,1	4	–	–	–,-,-	1,-,-
S9	R	23	4	3	2	–,-,-	–,-,-	6	5	4	–,-,-	–,-,-
S10	L	12	1	1	–	–,-,-	–,-,-	4	3	3	–,-,-	–,-,-
TOTAL		168	39	29	13	2,2,2	3,3,2	45	28	22	–,-,-	2,-,-

The numbers separated by commas correspond to AA, AS, AO or MA, MS, MO, respectively. Electrodes included are statistically significant at $p < .05$, FDR-corrected within participants. Hemi = hemisphere; TOT = total number of electrodes; AA = arithmetic condition active (relative to baseline); MS = arithmetic condition selective (relative to baseline and memory); AO = arithmetic condition only (arithmetic-selective and memory not active relative to baseline); MA = memory condition active (relative to baseline); MS = memory condition selective (relative to baseline and arithmetic); MO = memory condition only (memory selective and arithmetic not active relative to baseline); DecIN = decreased initial activity as a function of *min* operand; IncTO = increased total activity as a function of *min* operand.

Table 7. Selectivity and Modulation Related to the Recognition of Arabic Numerals in the VTC Channels that Showed Decreased Initial Activity as a Function of *Min* Operand

Participant	Hemi	Region	Numeral Active	Numeral Selective	Modulation by Numeral
S1	R	pITG	✓	–	–
S1	R	pITG	✓	–	–
S1	R	pITG	–	–	–
S2	L	pITG	✓	–	–
S2	L	aITG	–	–	–
S5	L	pITG	✓	–	–
S5	L	pITG	✓	–	–
S6	L	pITG	–	–	–
S8	R	pITG	✓	✓	–
S8	R	pITG	✓	–	–
S9	R	pITG	–	–	–

Numeral active, relative to baseline; Numeral selective, relative to baseline, Latin letters, and foreign letters. (✓) Statistically significant at $p <$ .05, FDR-corrected. Hemi = hemisphere.

operand and NUD as predictors. The effect of the *min* operand clearly dominated: It remained significant in 9 of 11 ITG sites ($p <$ .05, FDR-corrected). Crucially, the "number of unique digits" did not significantly explain unique variance in any of the ITG sites ($p >$ .6, FDR-corrected). Therefore, we can clearly refute this possible confound.

The absolute distance between the proposed result and the correct result also had a small, nonsignificant negative correlation with *min* operand ($\rho = -0.17$, $p = .113$) and is known to affect arithmetic verification (Ashcraft, 1992). To evaluate whether the observed ITG modulation originated from a distance effect at the verification stage, we again ran a multiple regression model with *min* operand and absolute deviant as predictors. Once again, the effect of *min* operand clearly dominated: It was unaffected in all 11 ITG sites ($p <$ .05, FDR-corrected). Crucially, the absolute distance did not significantly explain unique variance at any of the ITG sites ($p >$ .5, FDR-corrected).

A third variable that is known to affect calculation (Ashcraft, 1992) and was necessarily confounded with the size of the *min* operand is decade crossing, that is, whether the addition crosses a decade boundary such that the decade of the result is different from the decade of the first operand (e.g., $\underline{3}4 + 8 = \underline{4}2$). In this study, it is not trivial to completely disambiguate those two effects, the multiple regression suffers from multicollinearity, but we tested anyways. In the model with both *min* operand and decade crossing as predictors, the effect of *min* operand

remained significant in 4 of 11 channels in pITG ($p <$ .01). Importantly, decade crossing did not significantly explain unique variance in any of the ITG sites ($p >$ .3), and the βs were overall much more negative (stronger effect) for *min* operand as compared with decade crossing (mean *min* operand $= -0.385$, $SD = 0.138$; mean decade crossing $= -0.001$, $SD = 0.185$, $t(20) = -5.4840$, $p <$ .000).

In summary, those control analyses suggest that the modulation observed in the pITG is indeed due to arithmetic problem size/difficulty, which is primarily driven by the magnitude of the *min* operand. The design of the stimuli did not allow us to fully decorrelate the *min* operand from the decade crossing effect, and both variables may have contributed to problem difficulty, but the *min* effect seemed to be dominant.

Dissociation from RT

Finally, to verify if the parametric modulation by *min* operand directly translated to behavior and whether this effect was independent of other factors that influence RT, such as attention, decision-making, and motor preparation, we used multiple linear regression to model HFB activity as a function of both *min* operand and RT (Figure 5B and C). When regressing out the effect of RT, the initial activity at most pITG sites remained significantly modulated by *min* operand at 9 of the 10 observed sites. Conversely, once we regressed out the effect of RT from the total activity in aIPS and SPL, the effect of *min* operand completely vanished in all sites (Figure 5B). As shown in Figure 5C, the total activity in almost all VTC and LPC sites significantly correlated with RT, independent of *min* operand. Therefore, in contrast with the increase in total activity as a function of *min* operand observed in aIPS and SPL sites, which proved to be directly related behavior, the parametric decrease of the initial activity as a function of *min* operand observed in pITG was partially dissociated from RT, possibly indicating a role in the earlier stages of the calculation that does not directly translate into subsequent stages.

DISCUSSION

By recording electrophysiological signals directly from the human cortex with remarkable temporal and spatial resolution, we characterized the response selectivity and parametric modulation patterns in neuronal populations of the lateral parietal and ventral temporal cortices during mental arithmetic. Our results demonstrated a high degree of selectivity for calculations in a network composed of the aIPS and the SPL in the LPC and the pITG in the VTC, almost completely dissociated from the selectivity observed during sentence comprehension (memory condition), observed in the angular gyrus and STS and the medial inferior temporal cortex, known to be involved in language comprehension (Pallier et al., 2011) and

reading (Hannagan et al., 2015), respectively. This dissociation is in line with previous reported iEEG results (Hermes et al., 2017; Daitch et al., 2016), with a recent fMRI study that used an analogous task (Amalric & Dehaene, 2016), with a series of prior fMRI findings (Arsalidou & Taylor, 2011), and with studies that used intraoperative electrical stimulation (Semenza et al., 2017; Della Puppa et al., 2013).

All participants performed the addition task with high accuracy, and their RT patterns reflected the most widely replicated behavioral effect in cognitive arithmetic: the problem size effect (Zbrodoff & Logan, 2005; Ashcraft, 1992). More specifically, we found that the best predictor of RT and, therefore, problem size/difficulty was the smaller of the two operands (called *min*), corroborating several studies that used a variety of paradigms, such as production, verification, and number-to-position (Pinheiro-Chagas et al., 2017; Uittenhove et al., 2016; Barrouillet & Thevenot, 2013; Groen & Parkman, 1972). This result is also compatible with the original *min* model (Groen & Parkman, 1972) and with its recent variants, including the concept of "fast automated procedures" for scrolling on an ordered representation (Uittenhove et al., 2016; Barrouillet & Thevenot, 2013) or the hypothesis of a stepwise displacement on the "mental number line", starting with the *max* operand and incrementally adding the *min* operand (Pinheiro-Chagas et al., 2017). Nevertheless, the present results should not be seen as providing definitive support for "counting-based" or "fast compact procedures" models. The goal of this study was not to arbitrate between different cognitive models of mental arithmetic, and we used the *min* operand as a numerical index of problem size/difficulty, merely because it was by far the best predictor of RT.

Next, we investigated if, how, and when the *min* operand modulated the activity in the LPC and VTC arithmetic-selective regions. As predicted, we found several sites in aIPS and SPL in which the total HFB activity (integral of HFB power across the whole trial from stimuli onset to participant's RT) increased as a function of problem size/difficulty, indexed as the magnitude of the *min* operand, whereas the initial activity remained constant. These results replicate previous fMRI findings (Kanjlia et al., 2016; De Visscher et al., 2015; De Smedt et al., 2011; Molko et al., 2003; Dehaene et al., 1999), but with a much greater level of anatomical and temporal precision and at the single-participant level.

Importantly, once we regressed out the effect of RT, the modulation of total activity in aIPS and SPL by *min* operand vanished, suggesting that that the aIPS and SPL are engaged in the calculation process itself and are directly linked to behavioral RT modulations. One possibility is that aIPS and SPL may be involved in the slow accumulation of evidence needed to achieve a decision (Gonzalez et al., 2015; Tosoni, Galati, Romani, & Corbetta, 2008), in this case about the truth of an arithmetic problem. Future work could capitalize on the high signal-to-noise ratio and temporal and spatial resolution of

iEEG to test accumulation-of-evidence models (Dehaene, 2007; Gold & Shadlen, 2007), using simpler numerical tasks such as number comparison or single-digit arithmetic.

Note that in this study, LPC contained sites whose total HFB activity in a trial was positively correlated with *min* operand yet which were not selective for arithmetic processing (e.g., were active during both arithmetic and memory trials). Those sites might therefore have been engaged in sustained attention, decision-making, motor preparation, or some other nonarithmetic-related process.

Recent iEEG findings revealed the existence of neuronal populations in the pITG that selectively respond to Arabic numerals (NFA) as compared with other similar stimuli, such as letters (Shum et al., 2013). However, subsequent iEEG studies showed that responses to numerals in the VTC are more complex than what it was previously predicted by the triple-code model (Dehaene & Cohen, 1995) by revealing that, adjacent to the NFA, there are neuronal populations that respond to numerals more strongly (Hermes et al., 2017) or even exclusively (Daitch et al., 2016) when they are in the context of calculation, possibly reflecting top–down modulation coming from the LPC. Furthermore, recent fMRI studies showed that voxels around the pITG are also active for number processing in blind participants who learned to associated number shapes with sounds (Abboud, Maidenbaum, Dehaene, & Amedi, 2015) and when professional mathematicians evaluate high-level mathematical statements auditorily presented (Amalric & Dehaene, 2016). These results suggest that pITG might be involved in calculation beyond visual recognition of mathematical objects.

However, the precise role of pITG was not carefully examined, because none of the prior studies investigated if, how, and when activity in pITG is modulated by numerical features of the calculations. Our results showed a surprising and unpredicted new effect in several pITG sites: a parametrical decrease in the initial activity (within 1 sec of stimulus onset) as a function of problem size/ difficulty, whereas the total activity remained constant. This suggests that pITG engagement in multidigit calculation is directly linked to quantity-related features of calculations and do not simply reflect top–down attentional modulation or sustained working memory subserving regions that execute the actual computation. If that was the case, the total activity in pITG, as in the aIPS and SPL, should have increased as a function of *min* operand. Crucially, because fMRI is only sensitive to the activity integrated over a temporal window of several seconds, the initial modulation observed in pITG would be undetectable with fMRI. This may explain why previous fMRI studies did not observe modulation in the pITG by arithmetic problem size, but exclusively in a parietal-frontal network, including mainly the bilateral aIPS and SPL and the left inferior frontal gyrus (Kanjlia et al., 2016; Molko et al., 2003; Stanescu-Cosson et al., 2000).

The paradigm used in this study, which involves judging the correctness of a problem, is likely to involve

several processing stages: recognizing the numbers involved in the problem, computing the sum of the two operands, and comparing the sum with the proposed result. Although our study cannot explicitly separate the neural processes corresponding to these stages, it seems likely that the *min*-related activity observed in pITG sites is primarily related to an early stage because, first, the most salient effects are observed during the beginning of a trial and, second, the *min* effect remained at most sites even after regressing out the effect of RT, although we would expect the calculation and decision-related processes to be correlated with RT.

Why would pITG activity related to calculation decrease for more difficult problems? Simple arithmetic problems appear to induce a temporal concentration of activity into a fast and strong initial peak. Conversely, for more complex problems, the same total amount of activity appeared to be diluted in time. These findings suggest that pITG may index the difficulty or amount of evidence available for a calculation problem. In this respect, our findings, in a high-level semantic task, parallel the observations made during perceptual decision-making tasks, for instance, the fact that activity in middle temporal area indexes the amount of perceptual evidence for a motion-based decision and therefore varies inversely with task difficulty (Britten, Shadlen, Newsome, & Movshon, 1993). A possible alternative interpretation could be that the higher initial activity observed in the pITG for smaller *min* operands reflects tuning to more familiar symbols, because it is known that the frequency of number words and digits decrease as a function of numerosity (Dehaene & Mehler, 1992). However, an important argument against this interpretation is the fact that the pITG sites that showed a decreased initial activity as a function of *min* operand falls adjacent to, but not directly in, the NFA and do not show selective responses to isolated numerals as compared with other similar visual objects. Crucially, even the pITG sites that were active during Arabic digit recognition did not show any modulation by the magnitude of the numbers, that is, they equally responded to digits ranging from 1 to 9. Furthermore, as all elements of the addition were presented simultaneously in the screen, it is very unlikely that the pITG would be tuned to the frequency of only one of the elements, especially because the *min* operand appeared as the first operand in half of the trials and as the second operand in the other half. Another possibility is that pITG stores visual representations of the whole addition problem, as suggested by an early fMRI study (Rickard et al., 2000). In this case, the pITG modulation could potentially reflect the frequency of individual problem. Further studies, using a larger stimuli list and more adapted experimental design should try to arbitrate between these competing hypotheses.

Overall, we found a clear dissociation between the pattern of modulation by problem size/difficulty in LPC and VTC. However, a couple of sites in the LPC also showed significant decreased initial activity as a function of *min* operand, similar to the modulation observed in pITG. This might reflect the existence of functional connectivity between some neuronal populations in pITG and aIPS, as previously reported (Daitch et al., 2016). In this study, however, only a single participant had simultaneous coverage of VTC and LPC and exhibited distinct sites with decreased pITG initial activity and increased IPS total activity as a function of *min* operand. Consequently, we could not systematically investigate how the functional profiles of LPC and VTC differ within participants and, importantly, how these two distinct regions interact.

In summary, our results confirmed the selective engagement of aIPS and SPL in mental calculation and reveal an unexpected pattern of parametric modulation in pITG, possibly reflecting a role in the early identification of the difficulty/amount of evidence associated with a given computation. In the absence of reported bilateral focal lesions in the pITG region, its role in calculations remained unsuspected by previous neuropsychological studies (Cappelletti, 2015, for a recent review) and asks for a reevaluation of the neurocognitive models of arithmetic and acquired and developmental dyscalculia. Updated models should incorporate the pITG as an important hub for mental calculation, and any future studies on numerical cognition should include it as an ROI. More broadly, our results challenge the classical view of VTC as the last stage of the visual object categorization network and show that it contains regions crucially involved in mathematical processing.

Acknowledgments

REFERENCES

Abboud, S., Maidenbaum, S., Dehaene, S., & Amedi, A. (2015). A number-form area in the blind. *Nature Communications*, 6. https://doi.org/10.1038/ncomms7026

Amalric, M., & Dehaene, S. (2016). Origins of the brain networks for advanced mathematics in expert mathematicians. *Proceedings of the National Academy of Sciences, U.S.A.*, *113*, 4909–4917.

Arsalidou, M., & Taylor, M. J. (2011). Is 2+2=4? Meta-analyses of brain areas needed for numbers and calculations. *Neuroimage*, *54*, 2382–2393.

Ashcraft, M. H. (1992). Cognitive arithmetic: A review of data and theory. *Cognition*, *44*, 75–106.

Barrouillet, P., & Thevenot, C. (2013). On the problem size effect in small additions: Can we really discard any counting-based account? *Cognition*, *128*, 35–44.

Brainard, D. H. (1997). The Psychophysics Toolbox. *Spatial Vision*, *10*, 433–436.

Britten, K. H., Shadlen, M. N., Newsome, W. T., & Movshon, J. A. (1993). Responses of neurons in macaque MT to stochastic motion signals. *Visual Neuroscience*, *10*, 1157–1169.

Cappelletti, M. (2015). The neuropsychology of acquired number and calculation disorders. In R. Cohen-Kadosh & A. Dowker (Eds.), *The Oxford handbook of numerical cognition* (pp. 808–836). Oxford: Oxford University Press.

Daitch, A. L., Foster, B. L., Schrouff, J., Rangarajan, V., Kasikci, I., Gattas, S., et al. (2016). Mapping human temporal and parietal neuronal population activity and functional coupling during mathematical cognition. *Proceedings of the National Academy of Sciences, U.S.A.*, *113*, 201608434.

De Smedt, B., Holloway, I. D., & Ansari, D. (2011). Effects of problem size and arithmetic operation on brain activation during calculation in children with varying levels of arithmetical fluency. *Neuroimage*, *57*, 771–781.

De Visscher, A., Berens, S. C., Keidel, J. L., Noël, M., Bird, C. M., De Visscher, A., et al. (2015). The interference effect in arithmetic fact solving: An fMRI study. *Neuroimage*, *116*, 92–101.

Dehaene, S. (2007). Symbols and quantities in parietal cortex: Elements of a mathematical theory of number representation and manipulation. In P. Haggard, Y. Rossetti, & M. Kawato (Eds.), *Attention & performance XXII: Sensorimotor foundations of higher cognition* (pp. 527–574). Cambridge: Oxford University Press.

Dehaene, S., & Cohen, L. (1995). Towards an anatomical and functional model of number processing. *Mathematical Cognition*, *1*, 83–120.

Dehaene, S., & Mehler, J. (1992). Cross-linguistic regularities in the frequency of number words. *Cognition*, *43*, 1–29.

Dehaene, S., Piazza, M., Pinel, P., & Cohen, L. (2003). Three parietal circuits for number processing. *Cognitive Neuropsychology*, *20*, 487–506.

Dehaene, S., Spelke, E., Pinel, P., Stanescu, R., & Tsivkin, S. (1999). Sources of mathematical thinking: Behavioral and brain-imaging evidence. *Science*, *284*, 970–974.

Della Puppa, A., De Pellegrin, S., d'Avella, E., Gioffrè, G., Munari, M., Saladini, M., et al. (2013). Right parietal cortex and calculation processing: Intraoperative functional mapping of multiplication and addition in patients affected by a brain tumor. *Journal of Neurosurgery*, *119*, 1107–1111.

Foster, B. L., Rangarajan, V., Shirer, W. R., & Parvizi, J. (2015). Intrinsic and task-dependent coupling of neuronal population activity in human parietal cortex. *Neuron*, *86*, 578–590.

Gold, J. I., & Shadlen, M. N. (2007). The neural basis of decision making. *Annual Review of Neuroscience*, *30*, 535–574.

Gonzalez, A., Hutchinson, J. B., Uncapher, M. R., Chen, J., LaRocque, K. F., Foster, B. L., et al. (2015). Electrocorticography reveals the temporal dynamics of posterior parietal cortical activity during recognition memory decisions. *Proceedings of the National Academy of Sciences, U.S.A.*, *112*, 11066–11071.

Grill-Spector, K., & Weiner, K. S. (2014). The functional architecture of the ventral temporal cortex and its role in categorization. *Nature Reviews Neuroscience*, *15*, 536–548.

Groen, G. J., & Parkman, J. M. (1972). A chronometric analysis of simple addition. *Psychological Review*, *79*, 329–343.

Grotheer, M., Jeska, B., & Grill-Spector, K. (2018). A preference for mathematical processing outweighs the selectivity for Arabic numbers in the inferior temporal gyrus. *Neuroimage*, *175*, 188–200.

Hannagan, T., Amedi, A., Cohen, L., Dehaene-Lambertz, G., & Dehaene, S. (2015). Origins of the specialization for letters and numbers in ventral occipitotemporal cortex. *Trends in Cognitive Sciences*, *19*, 374–382.

Harvey, B. M., Ferri, S., & Orban, G. A. (2017). Comparing parietal quantity-processing mechanisms between humans and macaques. *Trends in Cognitive Sciences*, *21*, 779–793.

Harvey, B. M., Klein, B. P., Petridou, N., & Dumoulin, S. O. (2013). Topographic representation of numerosity in the human parietal cortex. *Science*, *341*, 1123–1126.

Hermes, D., Miller, K. J., Noordmans, H. J., Vansteensel, M. J., & Ramsey, N. F. (2010). Automated electrocorticographic electrode localization on individually rendered brain surfaces. *Journal of Neuroscience Methods*, *185*, 293–298.

Hermes, D., Rangarajan, V., Foster, B. L., King, J.-R., Kasikci, I., Miller, K. J., et al. (2017). Electrophysiological responses in the ventral temporal cortex during reading of numerals and calculation. *Cerebral Cortex*, *27*, 567–575.

Kanjlia, S., Lane, C., Feigenson, L., & Bedny, M. (2016). Absence of visual experience modifies the neural basis of numerical thinking. *Proceedings of the National Academy of Sciences, U.S.A.*, *113*, 201524982.

Knops, A., Thirion, B., Hubbard, E. M., Michel, V., & Dehaene, S. (2009). Recruitment of an area involved in eye movements during mental arithmetic. *Science*, *324*, 1583–1585.

Logothetis, N. K., Pauls, J., Augath, M., Trinath, T., & Oeltermann, A. (2001). Neurophysiological investigation of the basis of the fMRI signal. *Nature*, *412*, 150–157.

Manning, J. R., Jacobs, J., Fried, I., & Kahana, M. J. (2009). Broadband shifts in local field potential power spectra are correlated with single-neuron spiking in humans. *Journal of Neuroscience*, *29*, 13613–13620.

Menon, V., Rivera, S. M., White, C. D., Glover, G. H., & Reiss, A. L. (2000). Dissociating prefrontal and parietal cortex activation during arithmetic processing. *Neuroimage*, *12*, 357–365.

Molko, N., Cachia, A., Bruandet, M., Le Bihan, D., Cohen, L., & Dehaene, S. (2003). Functional and structural alterations of the intraparietal sulcus in a developmental dyscalculia of genetic origin. *Neuron*, *40*, 847–858.

Pallier, C., Devauchelle, A. D., & Dehaene, S. (2011). Cortical representation of the constituent structure of sentences. *Proceedings of the National Academy of Sciences, U.S.A.*, *108*, 2522–2527.

Parvizi, J., Jacques, C., Foster, B. L., Witthoft, N., Rangarajan, V., Weiner, K. S., et al. (2012). Electrical stimulation of human fusiform face-selective regions distorts face perception. *Journal of Neuroscience*, *32*, 14915–14920.

Piazza, M., Izard, V., Pinel, P., Le Bihan, D., & Dehaene, S. (2004). Tuning curves for approximate numerosity in the human intraparietal sulcus. *Neuron*, *44*, 547–555.

Piazza, M., Pinel, P., Le Bihan, D., & Dehaene, S. (2007). A magnitude code common to numerosities and number symbols in human intraparietal cortex. *Neuron*, *53*, 293–305.

Pinel, P., Dehaene, S., Rivière, D., & LeBihan, D. (2001). Modulation of parietal activation by semantic distance in a number comparison task. *Neuroimage*, *14*, 1013–1026.

Pinheiro-Chagas, P., Dotan, D., Piazza, M., & Dehaene, S. (2017). Finger tracking reveals the covert stages of mental arithmetic. *Open Mind: Discoveries in Cognitive Science*, *1*, 30–41.

Ray, S., & Maunsell, J. H. R. (2011). Different origins of gamma rhythm and high-gamma activity in macaque visual cortex. *PLoS Biology*, *9*, e1000610.

Rickard, T. C., Romero, S. G., Basso, G., Wharton, C., Flitman, S., & Grafman, J. (2000). The calculating brain: An fMRI study. *Neuropsychologia*, *38*, 325–335.

Semenza, C., Salillas, E., De Pallegrin, S., & Della Puppa, A. (2017). Balancing the 2 hemispheres in simple calculation: Evidence from direct cortical electrostimulation. *Cerebral Cortex*, *27*, 4806–4814.

Shum, J., Hermes, D., Foster, B. L., Dastjerdi, M., Rangarajan, V., Winawer, J., et al. (2013). A brain area for visual numerals. *Journal of Neuroscience*, *33*, 6709–6715.

Stanescu-Cosson, R., Pinel, P., van De Moortele, P. F., Le Bihan, D., Cohen, L., & Dehaene, S. (2000). Understanding dissociations in dyscalculia: A brain imaging study of the impact of number size on the cerebral networks for exact and approximate calculation. *Brain*, *123*, 2240–2255.

Tosoni, A., Galati, G., Romani, G. L., & Corbetta, M. (2008). Sensory-motor mechanisms in human parietal cortex underlie arbitrary visual decisions. *Nature Neuroscience*, *11*, 1446–1453.

Uittenhove, K., Thevenot, C., & Barrouillet, P. (2016). Fast automated counting procedures in addition problem solving: When are they used and why are they mistaken for retrieval? *Cognition*, *146*, 289–303.

Zbrodoff, J. N., & Logan, G. D. (2005). What everyone finds: The problem size effect. In J. I. D. Campbell (Ed.), *The handbook of mathematical cognition* (pp. 331–345). New York: Psychology Press.